HHS Public Access

Author manuscript

Neurobiol Aging. Author manuscript; available in PMC 2022 December 01.

Published in final edited form as:

Neurobiol Aging. 2021 December ; 108: 179–188. doi:10.1016/j.neurobiolaging.2021.09.002.

The association between hippocampal volume and memory in pathological aging is mediated by functional redundancy#

Stephanie Langella, Ph.D.[1], **Peter J. Mucha, Ph.D.**[2], **Kelly S. Giovanello, Ph.D.**[1,3], **Eran Dayan, Ph.D.**[3,4,*] **Alzheimer's Disease Neuroimaging Initiative**[**]

[1]Department of Psychology & Neuroscience, University of North Carolina at Chapel Hill, NC, 27599, USA

[2]Department of Mathematics, Dartmouth College, NH 03755, USA

[3]Biomedical Research Imaging Center, University of North Carolina at Chapel Hill, NC 27514, USA

[4]Department of Radiology, University of North Carolina at Chapel Hill, NC 27599, USA

Abstract

Hippocampal neurodegeneration, a primary component of Alzheimer's disease pathology, relates to poor cognition; however, the mechanisms underlying this relationship are not well understood. Using a sample of cognitively normal older adults and individuals with mild cognitive impairment, this study aims to determine the topological properties of functional networks accompanying hippocampal atrophy in aging, along with their association to cognition and clinical progression. We considered two conceptually differing topological properties: redundancy (the existence of alternative channels of functional commutation) and local efficiency (the efficiency of local information exchange). Hippocampal redundancy, but not local efficiency, mediated the association between low hippocampal volume and low memory in both the whole sample and in ß-amyloid positive participants. Additionally, participants with high hippocampal volume, redundancy, and memory clustered separately from those with low values on all three measures, with the latter group showing higher conversion rates to dementia within three years. Together,

[*]Corresponding author: Eran Dayan, Ph.D. 130 Mason Farm Road, Chapel Hill, NC 27599, USA. eran_dayan@med.unc.edu.

[**]Data used in preparation of this article were obtained from the Alzheimer's Disease Neuroimaging Initiative (ADNI) database (adni.loni.usc.edu). As such, the investigators within the ADNI contributed to the design and implementation of ADNI and/or provided data but did not participate in analysis or writing of this report. A complete listing of ADNI investigators can be found at: http://adni.loni.usc.edu/wp-content/uploads/how_to_apply/ADNI_Acknowledgement_List.pdf

Stephanie Langella, Conceptualization, Methodology, Formal analysis, Writing – original draft, Writing – review & editing, Peter J. Mucha, Methodology, Writing – review & editing, Kelly S. Giovanello, Conceptualization, Writing – review & editing, Eran Dayan, Conceptualization, Methodology, Formal analysis, Writing – original draft, Writing – review & editing, Supervision, Funding acquisition

[#]Neuroimaging Initiative (ADNI) database (adni.loni.usc.edu). As such, the investigators within the ADNI contributed to the design and implementation of ADNI and/or provided data but did not participate in analysis or writing of this report. A complete listing of ADNI investigators can be found at: http://adni.loni.usc.edu/wp-content/uploads/how_to_apply/ADNI_Acknowledgement_List.pdf

Declarations of Competing Interest

None

Submission declaration and verification

The submitted work describes original results which have not been published previously and are not under consideration for publication elsewhere.

these results demonstrate that reduced hippocampal redundancy is one mechanism through which hippocampal atrophy associates with memory impairment in healthy and pathological aging.

Keywords

Hippocampus; Atrophy; Aging; Memory; Mild Cognitive Impairment; Magnetic Resonance Imaging

1. Introduction

Alzheimer's disease (AD) characteristic neuropathology, extracellular plaque deposits of ß-amyloid (Aß) and neurofibrillary tangles of hyperphosphorylated tau, accumulates during both healthy aging and mild cognitive impairment (MCI), and is accompanied by neurodegeneration and cognitive decline (Jack et al., 2013). Neurodegeneration, though not specific to AD (Jack Jr et al., 2018), has critical effects on cognition (Apostolova et al., 2012; Barnes et al., 2009; Frankó and Joly, 2013; Jack et al., 2000; Morra et al., 2009). Hippocampal atrophy in particular has been consistently associated with worse memory performance in cognitively normal (CN) individuals and in pathological aging (Golomb et al., 1993; Grundman et al., 2002; Huang et al., 2019; Nathan et al., 2017; O'Shea et al., 2016; Peng et al., 2015). Higher rates of atrophy are observed in later AD stages and in individuals with progressive cognitive decline as compared to those who remain stable (Apostolova et al., 2012; Barnes et al., 2009; Frankó and Joly, 2013; Jack et al., 2000; Morra et al., 2009). However, the functional mechanisms through which atrophy relates to impaired cognition remain uncertain.

Our primary objective was to determine whether topological properties of functional brain networks underlie the relationship between atrophy and cognition in older adulthood. Focusing on the hippocampus as one of the earliest sites of AD pathology (Harris et al., 2010), we considered two theoretically opposing functional properties through which hippocampal volume may relate to memory function: redundancy versus efficiency (Fig. 1). Redundancy, present in numerous biological systems, provides robustness to the system in the event of failure of a specific element through the existence of alternative channels of communication (Billinton and Allan, 1992; Glassman, 1987; Navlakha et al., 2014; Tononi et al., 1999). On the other hand, local efficiency, an important property in small-world networks, refers to the efficiency of local information exchange, with higher local efficiency contributing to a lower cost of information flow (Achard and Bullmore, 2007; Latora and Marchiori, 2001; Rubinov and Sporns, 2010).

As a network property, redundancy is computed as the sum of direct and indirect paths (edges) between nodes in a network (Di Lanzo et al., 2012; Langella et al., 2021; Leistritz et al., 2013; Sadiq et al., 2021). Whole-brain redundancy declines in aging (Sadiq et al., 2021), whereas hippocampal redundancy specifically benefits memory in aging and is reduced in MCI (Langella et al., 2021). In contrast to redundancy's emphasis on indirect connections, local efficiency refers to the efficiency of communication between neighboring nodes (i.e., those with direct paths). Local efficiency is lower in older adults as an averaged whole-brain property, in specific functional networks (e.g., default mode network), and regionally

(e.g., hippocampus) (Achard and Bullmore, 2007; Cao et al., 2014; Geerligs et al., 2015). Therefore, we hypothesized that reduced redundancy or loss of local efficiency may underlie the relationship between hippocampal atrophy and cognitive impairment.

Secondly, we examined the moderating effects of Aß burden on these relationships. Higher Aß burden, a more specific AD biomarker (Jack Jr et al., 2018), is also related to memory impairment in healthy aging and MCI (Huang et al., 2019; Nathan et al., 2017). Therefore, individuals with greater pathological burden may show differential relationships between volume, function, and cognition. Finally, neurodegeneration itself is a poor predictor of conversion to AD, but we reasoned that the combination of structural, functional and cognitive measures may aid in predicting clinical outcomes. To that end, we assessed whether such a combination relates to subsequent dementia conversion. In sum, we aimed to elucidate whether topological network measures, either via robustness and redundancy or through efficiency of communication, are mechanisms through which atrophy impacts cognitive function.

2. Materials and Methods

Our analytic plan involved both hypothesis- and data-driven methods to test our primary aims. We first employed a hypothesis-driven approach by testing whether topological properties (derived from resting-state fMRI, rs-fMRI) mediated the relationship between volume (derived from structural MRI) and cognition. Next, we employed a data-driven approach, using k-means clustering on the variables of interest (structure, function, cognition) to ascertain whether results were consistent with our hypothesis-driven tests. Groups resulting from the clustering analysis were compared using survival analysis to evaluate differences in future clinical status, chosen to assess the clinical relevance of the selected variables.

2.1. Dataset

Data were obtained from the Alzheimer's Disease Neuroimaging Initiative (ADNI) database (adni.loni.usc.edu), a longitudinal multi-site study launched in 2003 and led by Principal Investigator Michael W. Weiner, MD. For up to date information, see www.adni-info.org. Study visits were approved by each site's local IRB. All participants provided informed consent. The following diagnostic inclusion criteria were established by ADNI: CN participants have no subjective memory concern or objective impairment, clinical dementia rating (CDR) = 0, Mini-Mental State Exam (MMSE) ≥ 24, non-depressed, non-MCI, non-demented; MCI participants have a subjective memory concern and objective memory impairment, CDR = 0.5, MMSE ≥ 24, no significant impairment in other cognitive domains, preserved activities of daily living, non-demented. CN and MCI participants from the ADNIGO/2 protocol between 60 and 90 years old with available rs-fMRI, structural MRI, florbetapir PET, and cognitive composite scores were included in this study. Functional and structural MRI images were collected on the same day, and PET images and cognitive measures were collected within three months of the MRI scan. The first available timepoint meeting these criteria was used for each participant (initial $n = 116$ participants).

2.2. MRI Data Acquisition and Processing

MRI scans were acquired on a 3 Tesla Philips Intera scanner (T1-weighted structural magnetization-prepared rapid gradient echo: flip angle = 9 degrees, TE = 3.1ms, TR = 6.8ms, sagittal plane, 1.0×1.0×1.2 mm^3; functional gradient echo: flip angle = 80 degrees, TE = 30ms, TR = 3000ms, 3.31×3.31×3.31 mm^3, eyes open). Image preprocessing was completed using the Conn toolbox, version 18b (Whitfield-Gabrieli and Nieto-Castanon, 2012), running on MATLAB (R2017b). Preprocessing included realignment and unwarping, correction of slice-timing, co-registration of functional to structural images, spatial normalization to MNI space, and segmentation of gray matter, white matter, and CSF. Motion outlier identification was used to identify and remove volumes with movement greater than 1.5mm or a global signal Z threshold of 7. Noise components from white matter and CSF along with six participant-motion parameters and their first order derivatives were included as nuisance variables. Signal frequencies below 0.008 Hz and above 0.09 Hz were removed using temporal band-pass filtering. Participants with greater than 50% of volumes removed due to excessive motion were excluded from subsequent analyses ($n = 12$).

2.3. Functional Network Construction and Calculation of Topological Measures

Functional time-series were extracted based on a functionally defined parcellation template composed of 300 distinct spherical regions of interest (ROIs), or nodes, encompassing cortical, subcortical, and cerebellar regions (Seitzman et al., 2020). Participant-level correlation matrices were constructed, in which edges represent Fisher Z transformed correlations between each node. Individual matrices were binarized at a range of densities retaining the top 2.5–25% of edges in each network, representing each participant's unweighted functional connectivity matrix. As we considered whole hippocampal volume as our variable of interest, network measures were calculated for each of the four hippocampal nodes included in the parcellation (encompassing bilateral anterior and posterior regions), then averaged to create one hippocampal ROI. To examine the specificity of any hippocampal effects, analyses were also conducted for the insula (comprised of eight nodes), a deep cortical structure which can be reliably segmented with T1 images, yet has slower rates of atrophy than do medial temporal lobe regions (Sluimer et al., 2009). Network measures were not related to total volume of white matter hyperintensities, nor did groups differ in underlying functional connectivity (see Supplementary Methods). A secondary thresholding procedure based on orthogonal minimum spanning trees was applied in order to determine the robustness of results to alternative thresholding methods, yielding consistent results to those from proportionally thresholded networks (see Supplementary Methods).

Redundancy: The path array, P, was calculated as the number of indirect and direct paths between each node pair (i, j) with path length l from each connectivity matrix. The redundancy matrix, R, was calculated as the sum of the paths between nodes i and j, up to maximum path length L, set to 4 (Langella et al., 2021; Sadiq et al., 2021). The average of each hippocampal nodal sum over j of R (hippocampal node, j) yielded the whole hippocampal ROI redundancy.

$$R(i,j) = \sum_{l=1}^{L} P(i,j,l)$$

Local Efficiency: Local efficiency, E_{local}, of the hippocampal ROI, i, was calculated as the average nodal efficiency among the neighboring nodes (where $L = 1$, and $L_{j,k}$ denotes the shortest path between nodes j,k) of node i, excluding itself, where N is the number of nodes in graph G_i, and G_i is the subgraph of G that includes all neighboring nodes of i. (Rubinov and Sporns, 2010)

$$E_{local} = \frac{1}{N_{G_i}\left(N_{G_i}-1\right)} \sum_{j,k \in G_i} \frac{1}{L_{j,k}}$$

2.4. Regional Brain Volume

Regional volume was available through ADNI. FreeSurfer v. 5.1 (Fischl, 2012) was used to segment anatomical MRI scans using the Desikan-Killany atlas and were manually checked for accuracy (full methods are available through ADNI). All structural MRI scans were taken on the same day as the rs-fMRI. Scans that failed the quality check were excluded from this analysis, as that indicates failed segmentation of the hippocampus (n = 2). Hippocampal volume was averaged across hemispheres as there were no hemispheric differences in either the whole sample, $t(101) = 0.16$, $p = .875$, or in MCI participants only, $t(74) = 0.18$, $p = .861$. The resulting average volume was normalized by dividing hippocampal volume by total intracranial volume and multiplied by 10^6 to retain the original scaling without influencing statistical test output. All participant scans passed the insula quality control check. As with the hippocampus, left and right hemisphere volumes were averaged, and resulting values were normalized using total intracranial volume.

2.5. Florbetapir PET

Florbetapir PET imaging was available through ADNI for participants within three months of their MRI scan dates. Mean florbetapir uptake was calculated for cortical gray matter regions, averaged to create a single cortical value, and normalized using a cerebellar reference region. Participants with normalized florbetapir uptake ≤1.11 were classified as Aß positive (Aß+), and those below 1.11 were classified as Aß negative (Aß−) (Clark et al., 2011; Joshi et al., 2012). Full methods are available through ADNI.

2.6. Cognitive Measures

We chose two cognitive processes as our outcome measures, in which deficits are observed throughout AD progression: memory, the earliest and primary cognitive deficit, and executive function (EF), which declines later in the disease (Arnaiz and Almkvist, 2003). Memory (primarily reflecting verbal recall and recognition) and EF were evaluated using composite measures calculated using an IRT framework (mean = 0, standard deviation = 1) (Crane et al., 2012; Gibbons et al., 2012) (see Supplementary Methods).

2.7. Statistical Analysis

Raw data were used for statistical analyses and were normalized for visualization. For brevity, statistical results and figures in the main text are reported using values averaged across densities. Results from each individual density are included in the Supplementary Materials to illustrate the robustness of findings across densities. Analyses were completed in both the whole-sample and in the MCI participants only. Across analyses, a significance level of $p < .05$ was used.

Group differences were analyzed in R using an independent samples *t*-test with equal variance assumed for two group comparisons, an ANOVA for comparisons involving more than two groups or when including covariates, and a chi-square test for dichotomous variables. Permutation ANCOVA was used for group comparisons of network measures because it is more robust to non-normality, implemented using the aovperm function from the permuco R package (Frossard and Renaud, 2019) (10,000 permutations, and with age, sex, and years of education as covariates). Linear regressions were estimated in R using the lm R function, with age, sex, and years of education included as covariates of no interest: (1) volume on cognition (memory, EF), (2) volume on network measure (redundancy, local efficiency), and (3) network measure on cognition. Resulting beta-weights were standardized using the lm.beta R function.

Mediation models were estimated using the mediation R package (Tingley et al., 2014) with volume as the predictor, cognition as the outcome, network measure as the mediator, and age, sex, and education as covariates of no interest. Effects were estimated using bootstrapping (10,000 simulations). In significant mediation models, Aß was included as a dichotomous moderator of the mediation, included in the path between the predictor and mediator. Indirect and direct effects of the model were conditionalized on Aß− and Aß+ separately. Indirect effects at each level were compared using bootstrapping (10,000 simulations).

K-means clustering was implemented in MATLAB. Values of *k* ranging from 2 to 8 were considered. The optimal *k* was determined using the silhouette method with 10,000 iterations and 10 simulations. Distance was measured using city block (Manhattan) distance, as it is less sensitive to outliers. Since different densities may result in different cluster solutions, rendering comparison across densities difficult, only the average density was used. Variables were normalized for clustering. Three-dimensional clustering was computed using hippocampal volume, memory, and redundancy. To assess the specific contribution of redundancy, we also completed two-dimensional clustering using memory and volume.

Groups resulting from the clustering procedure described above were compared with a survival analysis, testing the extent to which the groups differ in rates of conversion to dementia, using the survival (Therneau, 2020) and survminer (Kassambara et al., 2020) R packages, based on the Kaplan-Meier method to estimate survival probability. Groups were compared using a log-rank test. Participants were examined up to three years following the MRI visit to determine their conversion status. The earliest time point was selected if a participant did convert to dementia. If the participant did not convert, the latest available time point, up to three years post scan, was used (average follow-up time: 23.58 months for

the whole sample and 23.94 months for MCI only). In total, 12 participants converted to dementia.

3. Results

3.1. Association between hippocampal volume, memory, and topological network properties

The final sample consisted of 102 participants (Table 1). Diagnostic groups did not differ in hippocampal volume [$F(1,97) = 0.25$, $p = .621$]. The CN group had higher hippocampal redundancy than the MCI group [$F(1,97) = 7.48$, $p = .008$], but the groups did not differ in hippocampal local efficiency [$F(1, 97) = 0.12$, $p = .743$] (Table S1). Additionally, there was a positive relationship between redundancy and local efficiency, indicating that one does not come at the expense of the other (whole-sample: ß = 0.40, $p < .001$, $R^2_{adjusted} = .135$; MCI: ß = 0.38, $p = .001$, $R^2_{adjusted} = .127$; Table S2).

We first tested whether hippocampal volume was associated with our two cognitive measures. Lower hippocampal volume was associated with lower memory (whole-sample: ß = 0.38, $p < .001$, $R^2_{adjusted} = .230$; MCI: ß = 0.43, $p = .001$, $R^2_{adjusted} = .303$; Fig. 2a) but not to EF (whole-sample: ß = 0.17, $p = .102$, $R^2_{adjusted} = .218$; MCI: ß = 0.14, $p = .276$, $R^2_{adjusted} = .249$). Next, we examined the relationships of the topological network measures with volume and cognition (Tables 2, S3–S8). Lower hippocampal volume was related to lower redundancy, and in turn, lower hippocampal redundancy was related to worse memory performance (but not EF) (Figs. 2b, S1–S2). As with redundancy, lower hippocampal volume was related to lower local efficiency (Fig. 2c). However, local efficiency was not related to memory or EF.

3.2. Hippocampal redundancy underlies the hippocampal volume-memory relationship

We then estimated models to determine whether the topological properties mediated volume-cognition relationships (Tables 3, S9–S12). Hippocampal volume exerted a significant effect on memory through redundancy (whole-sample proportion mediated = 0.20, $p = .013$; MCI only proportion mediated = 0.17, $p = .039$; Figs. 2d, S2). Conversely, local efficiency did not mediate the hippocampal volume-memory relationship (Fig. 2e). Neither redundancy nor local efficiency mediated the relationship between volume and EF in either the whole sample or in MCI only, suggesting a specific role for hippocampal redundancy in memory ability.

The prior results suggest that participants with more risk for AD (i.e., low hippocampal volume), have accompanying low functional redundancy, which contributes to memory impairment. To test the hypothesis that individuals with higher rates of AD-pathology would show different relationships between structural and functional measures, we included Aß as a moderator in the volume-redundancy-memory mediation model (Tables S13, S14). In the whole sample, neither the Aß+ (indirect effect: ß = 1.44×10^{-4}, 95% CI[-9.16×10^{-7}, 3.44×10^{-4}], $p = .051$; direct effect: ß = 7.92×10^{-4}, 95% CI[3.85×10^{-4}, 1.26×10^{-3}], $p < .001$) nor Aß− (indirect effect: ß = 1.21×10^{-4}, 95% CI[-2.25×10^{-6}, 2.96×10^{-4}], $p = .054$; direct effect: ß = 1.25×10^{-4}, 95% CI[-3.65×10^{-4}, 6.82×10^{-4}], $p = .654$) effects

reached significance, and the indirect effects were not significantly different from each other ($p = .870$). When limiting to MCI participants, however, redundancy was a partial mediator of the volume-memory relationship for Aß+ participants (indirect effect: ß = 1.47×10^{-4}, 95% CI[4.28×10^{-6}, 4.00×10^{-4}], $p = .040$; direct effect: ß = 8.12×10^{-4}, 95% CI[4.08×10^{-4}, 1.24×10^{-3}], $p < .001$; proportion mediated: 0.15). Conversely, redundancy was not a significant mediator when estimating for Aß− participants (indirect effect: ß = 4.15×10^{-5}, 95% CI[-5.78×10^{-5}, 1.64×10^{-4}], $p = .351$; direct effect: ß = 8.85×10^{-5}, 95% CI[-4.53×10^{-4}, 6.97×10^{-4}], $p = .746$), suggesting that the functional redundancy mediation is specific to individuals harboring AD-pathology. However, the indirect effects for Aß+ and Aß− did not differ from one another ($p = .288$).

3.3. Low volume, redundancy, and memory predict subsequent dementia conversion

We sought to further explore the relationship between these variables using a data-driven approach, more specifically clustering participants based on hippocampal volume, redundancy, and memory. In our whole sample, a two cluster solution emerged, in which one cluster had low redundancy, volume, and memory (low RVM, $n = 50$), and the other had high values on all three variables (high RVM, $n = 52$). Each cluster was comprised of both CN and MCI participants, along with Aß− and Aß+ participants (Fig. 3a–b). The low RVM cluster had more MCI participants than the high RVM cluster [$X^2(1) = 6.63$, $p = .010$], but the clusters had similar proportions of Aß+ participants [$X^2(1) = 3.18$, $p = .075$]. Additionally, the low RVM group was older [$t(100) = 3.74$, $p < .001$] and had fewer years of education [$t(100) = 1.99$, $p = .049$].

The mediation results and cluster characteristics suggest that the combination of low hippocampal volume and low hippocampal redundancy is a risk factor for pathological aging. We sought additional evidence of this notion by examining rates of conversion to dementia in each of the clusters. Strikingly, no participants in the high RVM group converted to dementia, whereas all dementia conversions ($n = 12$) occurred in the low RVM group. The survival probability was thus lower in the low RVM cluster than in the high RVM cluster ($p < .001$) (Figs. 3d, S2). Critically, the two clusters did not differ in average follow-up time [$t(100) = 1.47$, $p = .145$].

Clustering just the MCI participants resulted in similar results, again finding a low RVM ($n = 35$) and a high RVM ($n = 40$) group. The clusters had similar proportions of Aß+ participants [$X^2(1) = 2.58$, $p = .108$]. The low RVM group was older than the high group [$t(73) = 3.43$, $p < .001$], but they had similar levels of education [$t(73) = 1.49$, $p = .141$]. Finally, individuals in the low RVM group were more likely to convert to dementia than those in the high RVM group ($p = .007$), with 10 of the 12 participants who converted to dementia clustering with low RVM. The two clusters did not differ in average follow-up time [$t(73) = 1.09$, $p = .281$].

To test the specific contribution of redundancy to the clustering approach reported above, we performed a post-hoc examination of participant clustering using only volume and memory. Because redundancy was positively related to hippocampal volume and memory (see section 3.1), the residuals from regressing volume on redundancy and from regressing memory on redundancy were used in the cluster analysis, thereby removing the effect of redundancy on

each variable. The removal of redundancy changed the results considerably, yielding four groups, between which survival probability did not differ (whole-sample: $p = .160$; MCI: $p = .120$). Further, the low VM group contained only four of the 12 converters in the whole sample and seven of the 12 in the MCI only participants, compared to the respective 12 and 10 converters in the analogous low RVM group.

3.4. Specificity of hippocampal atrophy

Finally, we examined the relationships between volume, redundancy, and memory in the insula, a deep cortical structure exhibiting a slower rate of atrophy in preclinical stages (Sluimer et al., 2009), to determine the specificity of hippocampal atrophy and function (Fig. 4; Tables S15–S17). Insular volume was not related to memory (whole-sample: ß = 0.14, $p = .140$, $R^2_{adjusted} = .144$; MCI: ß = 0.10, $p = .368$, $R^2_{adjusted} = .184$), nor to insular redundancy (whole-sample: ß = 0.11, $p = .315$, $R^2_{adjusted} = .010$; MCI: ß = 0.10, $p = .428$, $R^2_{adjusted} = .025$). Insular redundancy was not related to memory (whole-sample: ß = 0.08, $p = .396$, $R^2_{adjusted} = .131$; MCI: ß = 0.02, $p = .847$, $R^2_{adjusted} = .175$). Further, insular redundancy did not mediate the relationship between insular volume and memory in either the whole sample or MCI only (ps > .628).

4. Discussion

Despite widespread findings of hippocampal atrophy across healthy and pathological aging (Apostolova et al., 2012; Barnes et al., 2009; Frankó and Joly, 2013; Jack et al., 2000; Morra et al., 2009), the functional mechanisms through which hippocampal atrophy relates to impaired cognition remain uncertain. Our data suggest that hippocampal redundancy is one such mechanism. In CN and MCI older adults, we found that low hippocampal volume was related to low memory performance, which was mediated by low redundancy but not local efficiency. Data-driven clustering methods supported these findings, such that participants with low volume, redundancy, and memory clustered together and separately from those with high values on all three measures. Further, the low RVM cluster included all of the participants who subsequently converted to dementia. Consistent results were obtained when using an alternative thresholding method. Overall, these results provide evidence that low hippocampal redundancy underlies the relationship between hippocampal atrophy and memory impairment, and that this presentation of low structure, function, and cognition is a risk factor for conversion to dementia.

Our analysis focused on two topological network measures, redundancy and local efficiency, but only redundancy mediated the relationship between hippocampal volume and memory. Redundancy supports robustness in cellular and neural networks (Aittokallio and Schwikowski, 2006; Pitkow and Angelaki, 2017), and hippocampal functional redundancy is beneficial for memory and is reduced in pathological aging (Langella et al., 2021). Retaining hippocampal redundancy, then, may be neuroprotective in early stages of AD. Although a significant direct effect remained between hippocampal volume and memory, consistent with prior literature relating hippocampal atrophy to memory impairment (Golomb et al., 1993; Grundman et al., 2002; Huang et al., 2019; Nathan et al., 2017; O'Shea et al., 2016; Peng et al., 2015), the significant indirect effect through redundancy indicates

that memory impairment is not solely affected by volume loss itself; rather, this effect is partially explained by changes in hippocampal functional topology- namely lower redundancy. Interventions targeting hippocampal redundancy, therefore, may mitigate age-related cognitive decline. Such implications should be probed by testing to what degree redundancy can be increased in older adulthood, for example via lifestyle interventions or other modifiable factors known to affect brain health (Bugg and Head, 2011; Karatsoreos and McEwen, 2013; Ma et al., 2017; Olson et al., 2006; Piras et al., 2011; Tost et al., 2015; Wenger and Lövdén, 2016). Significant mediation effects were observed in both our combined sample as well as in just MCI participants. However, only in MCI was there evidence that the role of redundancy may differ as a result of Aß burden. Although the difference between Aß+ and Aß− effects did not reach significance, mediation was significant only for Aß+ participants, providing initial evidence that redundancy contributes to low memory in individuals with greater risk for developing AD (e.g., individuals with MCI who are Aß+), but exerts no effect in less impaired groups. The loss of hippocampal redundancy may accompany the accumulation of disease pathology. Future work should further probe potential differences as a function of pathological burden.

Our results also demonstrate a specificity to the role of hippocampal redundancy. Significant mediation by redundancy was only observed for the association of memory with hippocampal atrophy, not for EF. Whole-brain redundancy, on the other hand, supports EF in healthy adults (Sadiq et al., 2021). Though hippocampal function is implicated widely in cognition (Shohamy and Turk-Browne, 2013), given its primary involvement in mnemonic processes (Clark and Squire, 2013; Eichenbaum, 2017), our findings show that regional measures of redundancy appear to be selective in their effects. Additionally, insular redundancy did not mediate a relationship between insular volume and cognition, suggesting a relatively specific effect of the hippocampus in healthy and early pathological aging.

The finding of low and high RVM clusters in our dataset support our mediation findings that low structure, function, and cognition accompany each other. Further, the combination of low values on all three variables represents a risk state, with a higher proportion of individuals subsequently converting to dementia. However, when clustering on volume and memory, and equating redundancy, a more complex four-cluster solution emerged with ill-defined risk groups. The low VM cluster did not capture the high proportion of conversions that was achieved when including functional redundancy. Indeed, hippocampal neurodegeneration itself is not specific to AD (Jack Jr et al., 2018), and atrophy is common in healthy aging (Daugherty et al., 2016). In our sample, low hippocampal volume was a poor predictor of subsequent dementia conversion, but when accompanied by hippocampal redundancy, prediction substantially improves.

This study has several limitations. Our sample consisted of disproportionately more participants with MCI ($n = 75$) than CN ($n = 27$) individuals. To address this limitation, analyses were repeated using just MCI participants, with results supporting the same conclusions. However, we did not have a large enough CN sample to repeat the analyses in just CN participants. The hippocampal volume available for this sample was calculated using automated segmentation through Freesurfer, though manual tracing is currently the gold standard to minimize bias in estimates (Schmidt et al., 2018). To mitigate this

issue, only participants who passed ADNI's comprehensive quality control procedures were included in this study, though newer methods for hippocampal segmentation should be used to support the current findings. Additionally, the markers of interest were examined cross-sectionally, precluding longitudinal assessment of hippocampal atrophy or Aß accumulation. Future work should also employ longitudinal assessment of functional hippocampal redundancy to elucidate whether redundancy is malleable across healthy and pathology aging, such as in response to neuropathology.

In sum, we find that hippocampal redundancy underlies the relationship between low hippocampal volume and poor memory performance. Although neurodegeneration is a non-specific risk factor for AD (Jack Jr et al., 2018), by including this functional correlate of hippocampal atrophy, the ability to differentiate between stable and converter participants is improved. Topological network properties are thus critical in understanding the link between atrophy and cognitive impairment in preclinical older adults.

Supplementary Material

Refer to Web version on PubMed Central for supplementary material.

Acknowledgments

We thank Dr. Fabrizio De Vico Fallani for sharing MATLAB code to calculate redundancy.

Funding

Research reported in this publication was supported by the National Institute On Aging of the National Institutes of Health under Award Number R01AG062590. The content is solely the responsibility of the authors and does not necessarily represent the official views of the National Institutes of Health. Data collection and sharing for this project was funded by the Alzheimer's Disease Neuroimaging Initiative (ADNI) (National Institutes of Health Grant U01 AG024904) and DOD ADNI (Department of Defense award number W81XWH-12-2-0012). ADNI is funded by the National Institute on Aging, the National Institute of Biomedical Imaging and Bioengineering, and through generous contributions from the following: AbbVie, Alzheimer's Association; Alzheimer's Drug Discovery Foundation; Araclon Biotech; BioClinica, Inc.; Biogen; Bristol-Myers Squibb Company; CereSpir, Inc.; Cogstate; Eisai Inc.; Elan Pharmaceuticals, Inc.; Eli Lilly and Company; EuroImmun; F. Hoffmann-La Roche Ltd and its affiliated company Genentech, Inc.; Fujirebio; GE Healthcare; IXICO Ltd.; Janssen Alzheimer Immunotherapy Research & Development, LLC.; Johnson & Johnson Pharmaceutical Research & Development LLC.; Lumosity; Lundbeck; Merck & Co., Inc.; Meso Scale Diagnostics, LLC.; NeuroRx Research; Neurotrack Technologies; Novartis Pharmaceuticals Corporation; Pfizer Inc.; Piramal Imaging; Servier; Takeda Pharmaceutical Company; and Transition Therapeutics. The Canadian Institutes of Health Research is providing funds to support ADNI clinical sites in Canada. Private sector contributions are facilitated by the Foundation for the National Institutes of Health (www.fnih.org). The grantee organization is the Northern California Institute for Research and Education, and the study is coordinated by the Alzheimer's Therapeutic Research Institute at the University of Southern California. ADNI data are disseminated by the Laboratory for Neuro Imaging at the University of Southern California.

Data Availability

Raw image and cognitive data are available at adni.loni.usc.edu. Processed data and code will be made available upon reasonable request to the corresponding author.

Abbreviations

AD	Alzheimer's disease
CN	cognitively normal

MCI	mild cognitive impairment
Aß	beta-amyloid
EF	executive function

References

Achard S, Bullmore E, 2007. Efficiency and Cost of Economical Brain Functional Networks. PLOS Comput. Biol. 3, e17. [PubMed: 17274684]

Aittokallio T, Schwikowski B, 2006. Graph-based methods for analysing networks in cell biology. Brief. Bioinform. 7, 243–255. 10.1093/bib/bbl022 [PubMed: 16880171]

Apostolova LG, Green AE, Babakchanian S, Hwang KS, Chou Y-Y, Toga AW, Thompson PM, 2012. Hippocampal atrophy and ventricular enlargement in normal aging, mild cognitive impairment (MCI), and Alzheimer Disease. Alzheimer Dis. Assoc. Disord. 26, 17–27. 10.1097/WAD.0b013e3182163b62 [PubMed: 22343374]

Arnaiz E, Almkvist O, 2003. Neuropsychological features of mild cognitive impairment and preclinical alzheimer's disease. Acta Neurol. Scand. 107, 34–41.

Barnes J, Bartlett JW, van de Pol LA, Loy CT, Scahill RI, Frost C, Thompson P, Fox NC, 2009. A meta-analysis of hippocampal atrophy rates in Alzheimer's disease. Neurobiol. Aging 30, 1711–1723. 10.1016/j.neurobiolaging.2008.01.010 [PubMed: 18346820]

Billinton R, Allan RN, 1992. Reliability Evaluation of Engineering Systems, Springer. Boston. 10.1007/978-1-4899-0685-4

Bugg JM, Head D, 2011. Exercise moderates age-related atrophy of the medial temporal lobe. Neurobiol. Aging 32, 506–514. 10.1016/j.neurobiolaging.2009.03.008 [PubMed: 19386382]

Cao M, Wang J-H, Dai Z-J, Cao X-Y, Jiang L-L, Fan F-M, Song X-W, Xia M-R, Shu N, Dong Q, Milham MP, Castellanos FX, Zuo X-N, He Y, 2014. Topological organization of the human brain functional connectome across the lifespan. Dev. Cogn. Neurosci. 7, 76–93. 10.1016/j.dcn.2013.11.004 [PubMed: 24333927]

Clark CM, Schneider JA, Bedell BJ, Beach TG, Bilker WB, Mintun MA, Pontecorvo MJ, Hefti F, Carpenter AP, Flitter ML, Krautkramer MJ, Kung HF, Coleman RE, Doraiswamy PM, Fleisher AS, Sabbagh MN, Sadowsky CH, Reiman PEM, Zehntner SP, Skovronsky DM, 2011. Use of florbetapir-PET for imaging β-amyloid pathology. JAMA - J. Am. Med. Assoc. 305, 275–283. 10.1001/jama.2010.2008

Clark RE, Squire LR, 2013. Similarity in form and function of the hippocampus in rodents, monkeys, and humans. Proc. Natl. Acad. Sci. U. S. A. 110, 10365–10370. 10.1073/pnas.1301225110 [PubMed: 23754372]

Crane PK, Carle A, Gibbons LE, Insel P, Mackin RS, Gross A, Jones RN, Mukherjee S, Curtis SM, Harvey D, Weiner M, Mungas D, Initiative, for the A.D.N., 2012. Development and assessment of a composite score for memory in the Alzheimer's Disease Neuroimaging Initiative (ADNI). Brain Imaging Behav. 6, 502–516. 10.1007/s11682-012-9186-z [PubMed: 22782295]

Daugherty AM, Bender AR, Raz N, Ofen N, 2016. Age Differences in Hippocampal Subfield Volumes from Childhood to Late Adulthood. Hippocampus 26, 220–228. 10.1002/hipo.22517. [PubMed: 26286891]

Di Lanzo C, Marzetti L, Zappasodi F, De Vico Fallani F, Pizzella V, 2012. Redundancy as a graph-based index of frequency specific MEG functional connectivity. Comput. Math. Methods Med. 2012, 1–9. 10.1155/2012/207305

Eichenbaum H, 2017. On the Integration of Space, Time, and Memory. Neuron 95, 1007–1018. 10.1016/j.neuron.2017.06.036 [PubMed: 28858612]

Fischl B, 2012. FreeSurfer. Neuroimage 62, 774–781. [PubMed: 22248573]

Frankó E, Joly O, 2013. Evaluating Alzheimer's Disease Progression Using Rate of Regional Hippocampal Atrophy. PLoS One 8, 1–11. 10.1371/journal.pone.0071354

Frossard J, Renaud O, 2019. permuco: Permutation Tests for Regression, (Repeated Measures) ANOVA/ANCOVA and Comparison of Signals.

Geerligs L, Renken RJ, Saliasi E, Maurits NM, Lorist MM, 2015. A Brain-Wide Study of Age-Related Changes in Functional Connectivity. Cereb. Cortex 25, 1987–1999. 10.1093/cercor/bhu012 [PubMed: 24532319]

Gibbons LE, Carle AC, Mackin RS, Harvey D, Mukherjee S, Insel P, Curtis SM, Mungas D, Crane PK, Initiative, for the A.D.N., 2012. A composite score for executive functioning, validated in Alzheimer's Disease Neuroimaging Initiative (ADNI) participants with baseline mild cognitive impairment. Brain Imaging Behav. 6, 517–527. 10.1007/s11682-012-9176-1 [PubMed: 22644789]

Glassman RB, 1987. An hypothesis about redundancy and reliability in the brains of higher species: Analogies with genes, internal organs, and engineering systems. Neurosci. Biobehav. Rev. 11, 275–285. 10.1016/S0149-7634(87)80014-3 [PubMed: 3684057]

Golomb J, de Leon MJ, Kluger A, George AE, Tarshish C, Ferris SH, 1993. Hippocampal atrophy in aging: An association with recent memory impairment. JAMA Neurol. 50, 967–973.

Grundman M, Sencakova D, Jack CR, Petersen RC, Kim HT, Schultz A, Weiner MF, DeCarli C, DeKosky ST, Van Dyck C, Thomas RG, Thal LJ, 2002. Brain MRI hippocampal volume and prediction of clinical status in a mild cognitive impairment trial. J. Mol. Neurosci. 19, 23–27. 10.1007/s12031-002-0006-6 [PubMed: 12212787]

Harris JA, Devidze N, Verret L, Ho K, Halabisky B, Thwin MT, Kim D, Hamto P, Lo I, Yu G, Palop JJ, Masliah E, Mucke L, 2010. Transsynaptic progression of amyloid-induced neuronal dysfunction within the entorhinal-hippocampal network. Neuron 68, 428–441. 10.1016/j.neuron.2010.10.020 [PubMed: 21040845]

Huang K-L, Hsiao I-T, Kuo H-C, Hsieh C-J, Hsieh Y-C, Wu Y-M, Wey S-P, Yen T-C, Lin K-J, Huang C-C, 2019. Correlation between visual association memory test and structural changes in patients with Alzheimer's disease and amnestic mild cognitive impairment. J. Formos. Med. Assoc. 118, 1325–1332. 10.1016/j.jfma.2018.12.001 [PubMed: 30579663]

Jack CR, Knopman DS, Jagust WJ, Petersen RC, Weiner MW, Aisen PS, Shaw LM, Vemuri P, Wiste HJ, Weigand SD, Lesnick TG, Pankratz VS, Donohue MC, Trojanowski JQ, 2013. Tracking pathophysiological processes in Alzheimer's disease: An updated hypothetical model of dynamic biomarkers. Lancet Neurol. 12, 207–216. 10.1016/S1474-4422(12)70291-0 [PubMed: 23332364]

Jack CR, Petersen RC, Xu Y, O'Brien PC, Smith GE, Ivnik RJ, Boeve BF, Tangalos EG, Kokmen E, 2000. Rates of hippocampal atrophy correlate with change in clinical status in aging and AD. Neurology 55, 484–489. 10.1212/wnl.55.4.484 [PubMed: 10953178]

Jack CR Jr, Bennett DA, Blennow K, Carrillo MC, Dunn B, Budd Haeberlein S, Holtzman DM, Jagust W, Jessen F, Karlawish J, Liu E, Luis Molinuevo J, Montine T, Phelps C, Rankin KP, Rowe CC, Scheltens P, Siemers E, Snyder HM, Sperling R, Dement Author manuscript, A., 2018. NIA-AA Research Framework: Toward a biological definition of Alzheimer's disease. Alzheimers Dement 14, 535–562. 10.1016/j.jalz.2018.02.018.NIA-AA [PubMed: 29653606]

Joshi AD, Pontecorvo MJ, Clark CM, Carpenter AP, Jennings DL, Sadowsky CH, Adler LP, Kovnat KD, Seibyl JP, Arora A, Saha K, Burns JD, Lowrey MJ, Mintun MA, Skovronsky DM, 2012. Performance characteristics of amyloid PET with florbetapir F 18 in patients with Alzheimer's disease and cognitively normal subjects. J. Nucl. Med. 53, 378–384. 10.2967/jnumed.111.090340 [PubMed: 22331215]

Karatsoreos IN, McEwen BS, 2013. Resilience and vulnerability: a neurobiological perspective. F1000Prime Rep. 5, 13. 10.12703/P5-13 [PubMed: 23710327]

Kassambara A, Kosinski M, Biecek P, Fabian S, 2020. survminer: Drawing survival curves using "ggplot2."

Langella S, Sadiq MU, Mucha PJ, Giovanello KS, Dayan E, 2021. Lower functional hippocampal redundancy in mild cognitive impairment. Transl. Psychiatry 11. 10.1038/s41398-020-01166-w [PubMed: 33414382]

Latora V, Marchiori M, 2001. Efficient behavior of small-world networks. Phys. Rev. Lett. 87, 198701. 10.1103/PhysRevLett.87.198701 [PubMed: 11690461]

Leistritz L, Weiss T, Bär K-J, De VicoFallani F, Babiloni F, Witte H, Lehmann T, 2013. Network Redundancy Analysis of Effective Brain Networks; a Comparison of Healthy Controls and Patients with Major Depression. PLoS One 8, e60956. [PubMed: 23637778]

Ma C-L, Ma X-T, Wang J-J, Liu H, Chen Y-F, Yang Y, 2017. Physical exercise induces hippocampal neurogenesis and prevents cognitive decline. Behav. Brain Res. 317, 332–339. 10.1016/j.bbr.2016.09.067 [PubMed: 27702635]

Morra JH, Tu Z, Apostolova LG, Green AE, Avedissian C, Madsen SK, Parikshak N, Toga AW, Jack CR Jr, Schuff N, Weiner MW, Thompson PM, Initiative, A.D.N., 2009. Automated mapping of hippocampal atrophy in 1-year repeat MRI data from 490 subjects with Alzheimer's disease, mild cognitive impairment, and elderly controls. Neuroimage 45, S3–S15. 10.1016/j.neuroimage.2008.10.043 [PubMed: 19041724]

Nathan PJ, Lim YY, Abbott R, Galluzzi S, Marizzoni M, Babiloni C, Albani D, Bartres-Faz D, Didic M, Farotti L, Parnetti L, Salvadori N, Müller BW, Forloni G, Girtler N, Hensch T, Jovicich J, Leeuwis A, Marra C, Molinuevo JL, Nobili F, Pariente J, Payoux P, Ranjeva JP, Rolandi E, Rossini PM, Schönknecht P, Soricelli A, Tsolaki M, Visser PJ, Wiltfang J, Richardson JC, Bordet R, Blin O, Frisoni GB, 2017. Association between CSF biomarkers, hippocampal volume and cognitive function in patients with amnestic mild cognitive impairment (MCI). Neurobiol. Aging 53, 1–10. 10.1016/j.neurobiolaging.2017.01.013 [PubMed: 28189924]

Navlakha S, He X, Faloutsos C, Bar-Joseph Z, 2014. Topological properties of robust biological and computational networks. J. R. Soc. Interface 11, 20140283. 10.1098/rsif.2014.0283 [PubMed: 24789562]

O'Shea A, Cohen R, Porges E, Nissim N, Woods A, 2016. Cognitive Aging and the Hippocampus in Older Adults. Front. Aging Neurosci. 8, 298. 10.3389/fnagi.2016.00298 [PubMed: 28008314]

Olson AK, Eadie BD, Ernst C, Christie BR, 2006. Environmental enrichment and voluntary exercise massively increase neurogenesis in the adult hippocampus via dissociable pathways. Hippocampus 16, 250–260. 10.1002/hipo.20157 [PubMed: 16411242]

Peng G-P, Feng Z, He F-P, Chen Z-Q, Liu X-Y, Liu P, Luo B-Y, 2015. Correlation of Hippocampal Volume and Cognitive Performances in Patients with Either Mild Cognitive Impairment or Alzheimer's disease. CNS Neurosci. Ther. 21, 15–22. 10.1111/cns.12317 [PubMed: 25146658]

Piras F, Cherubini A, Caltagirone C, Spalletta G, 2011. Education mediates microstructural changes in bilateral hippocampus. Hum. Brain Mapp. 32, 282–289. 10.1002/hbm.21018 [PubMed: 20336658]

Pitkow X, Angelaki DE, 2017. Inference in the brain: Statistics flowing in redundant population codes. Neuron 94, 943–953. 10.1016/j.neuron.2017.05.028 [PubMed: 28595050]

Rubinov M, Sporns O, 2010. Complex network measures of brain connectivity: Uses and interpretations. Neuroimage 52, 1059–1069. 10.1016/j.neuroimage.2009.10.003 [PubMed: 19819337]

Sadiq MU, Langella S, Giovanello KS, Mucha PJ, Dayan E, 2021. Accrual of functional redundancy along the lifespan and its effects on cognition. Neuroimage 229, 117737. 10.1016/j.neuroimage.2021.117737 [PubMed: 33486125]

Schmidt MF, Storrs JM, Freeman KB, Jack CR, Turner ST, Griswold ME, Mosley TH, 2018. A comparison of manual tracing and FreeSurfer for estimating hippocampal volume over the adult lifespan. Hum. Brain Mapp. 39, 2500–2513. 10.1002/hbm.24017 [PubMed: 29468773]

Seitzman BA, Gratton C, Marek S, Raut RV, Dosenbach NUF, Schlaggar BL, Petersen SE, Greene DJ, 2020. A set of functionally-defined brain regions with improved representation of the subcortex and cerebellum. Neuroimage 206. 10.1016/j.neuroimage.2019.116290

Shohamy D, Turk-Browne NB, 2013. Mechanisms for widespread hippocampal involvement in cognition. J. Exp. Psychol. Gen. 142, 1159–1170. 10.1037/a0034461 [PubMed: 24246058]

Sluimer JD, van der Flier WM, Karas GB, van Schijndel R, Barnes J, Boyes RG, Cover KS, Olabarriaga SD, Fox NC, Scheltens P, Vrenken H, Barkhof F, 2009. Accelerating regional atrophy rates in the progression from normal aging to Alzheimer's disease. Eur. Radiol. 19, 2826. 10.1007/s00330-009-1512-5 [PubMed: 19618189]

Therneau T, 2020. A package for survival analysis in R.

Tingley D, Yamamoto T, Hirose K, Keele L, Imai K, 2014. mediation: R package for causal mediation analysis. J. Stat. Softw. 59, 1–38. [PubMed: 26917999]

Tononi G, Sporns O, Edelman GM, 1999. Measures of degeneracy and redundancy in biological networks. Proc. Natl. Acad. Sci. U. S. A. 96, 3257–3262. 10.1073/pnas.96.6.3257 [PubMed: 10077671]

Tost H, Champagne FA, Meyer-Lindenberg A, 2015. Environmental influence in the brain, human welfare and mental health. Nat. Neurosci. 18, 1421–1431. 10.1038/nn.4108 [PubMed: 26404717]

Wenger E, Lövdén M, 2016. The Learning Hippocampus: Education and Experience-Dependent Plasticity. Mind, Brain, Educ. 10, 171–183. 10.1111/mbe.12112

Whitfield-Gabrieli S, Nieto-Castanon A, 2012. Conn: A functional connectivity toolbox for correlated and anticorrelated brain networks. Brain Connect. 2, 125–141. 10.1089/brain.2012.0073 [PubMed: 22642651]

Highlights

- Low hippocampal volume is associated with low memory in aging
- Hippocampal functional redundancy mediates the volume-memory relationship
- Hippocampal local efficiency is not related to volume-memory association
- Low hippocampal volume, redundancy, and memory predict future dementia conversion

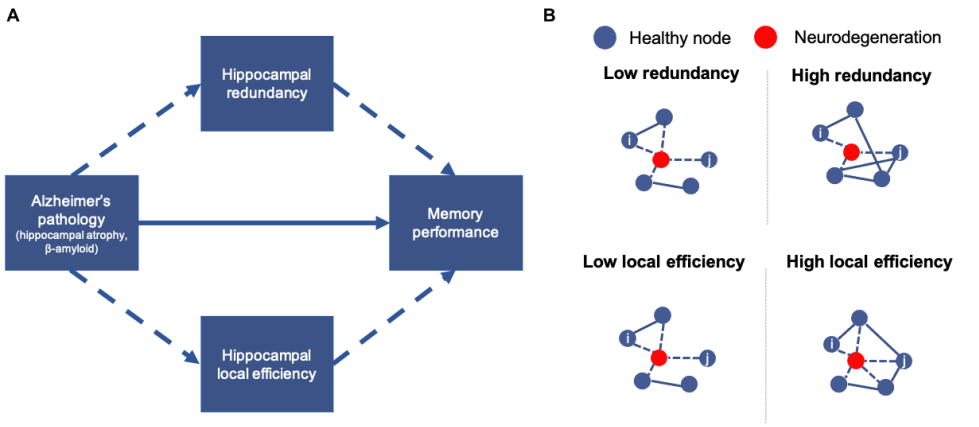

Figure 1. Study hypotheses.

A. Hypothesized mechanism through which hippocampal atrophy relates to memory impairment. **B**. Depiction of topological properties considered. In low redundancy or low local efficiency networks, degeneration of a node results in no paths between nodes *i,j.* In high redundancy and high local efficiency networks, alternate paths exist between nodes *i,j.*

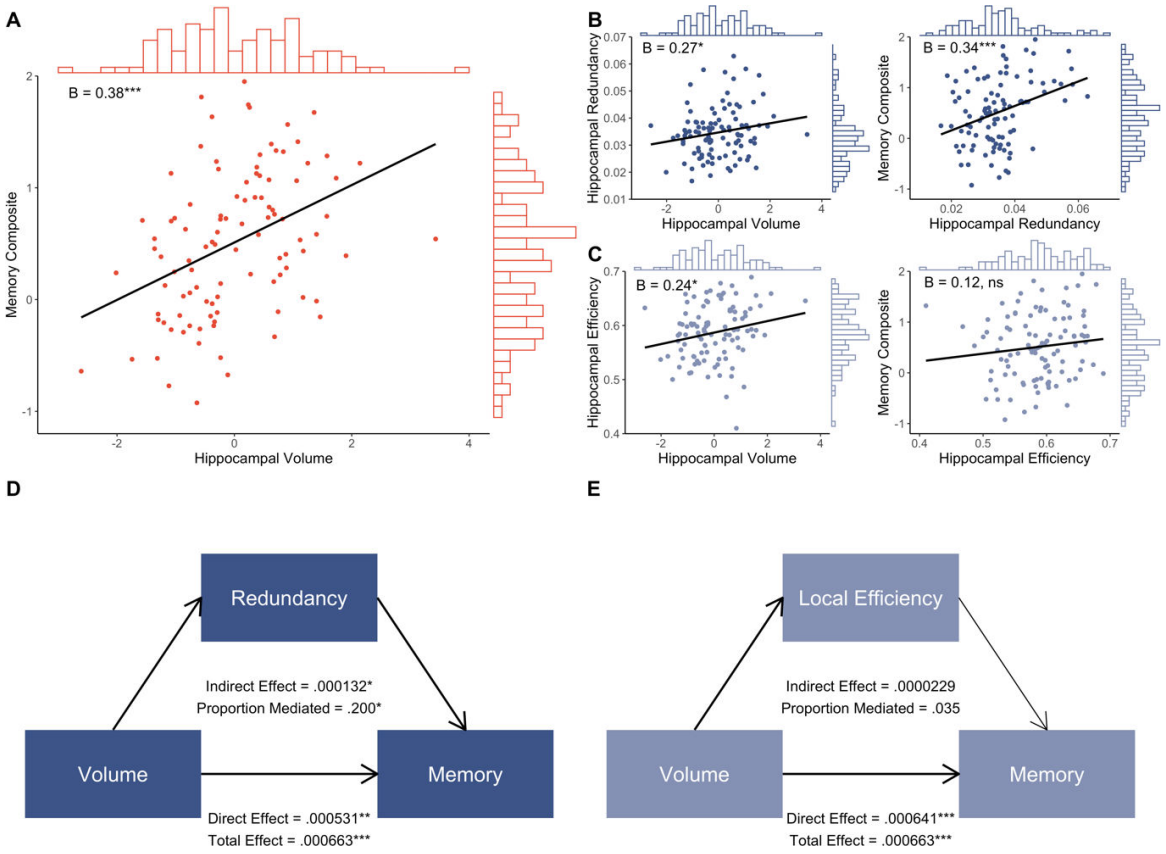

Figure 2. Relationships between hippocampal volume, topological network measures, and memory.

A. Whole-sample regression of hippocampal volume on memory composite score, with histograms showing distribution of variable values and inset standardized beta coefficients. **B.** Whole-sample regression of hippocampal volume on hippocampal redundancy, and of hippocampal redundancy on memory composite score, with histograms showing distribution of variable values and inset standardized beta coefficients. **C.** Whole-sample regression of hippocampal volume on hippocampal local efficiency, and of hippocampal local efficiency on memory composite score, with histograms showing distribution of variable values and inset standardized beta coefficients. **D.** Mediation results from hippocampal volume-redundancy-memory model. Bold lines denote significant paths. **E.** Mediation results from volume-local efficiency-memory model. Bold lines denote significant paths. *$p < .05$, **$p < .01$, ***$p < .001$

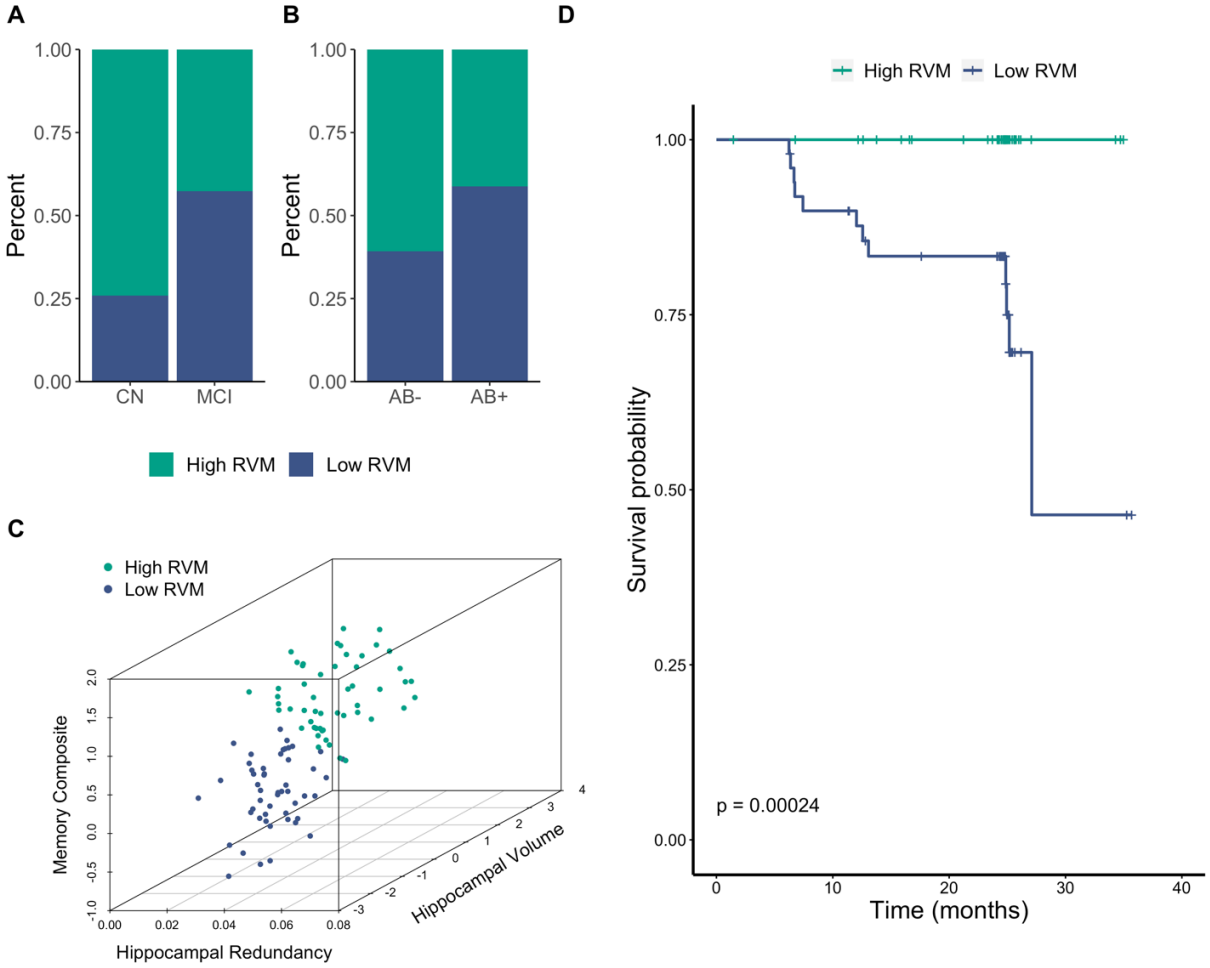

Figure 3. Characteristics of three-dimensional *K*-means clustering solution groups.

A. Percent of CN and MCI participants within each cluster. **B.** Percent of Aß− and Aß+ participants within each cluster. **C.** Scatterplot showing the relationship between hippocampal redundancy, hippocampal volume, and memory in each cluster. **D.** Survival probability for each cluster over time. Vertical drop in curve indicates a conversion to dementia. Tick marks represent censoring of a participant (i.e., final timepoint). RVM = redundancy, volume, memory; CN = cognitively normal; MCI = mild cognitive impairment

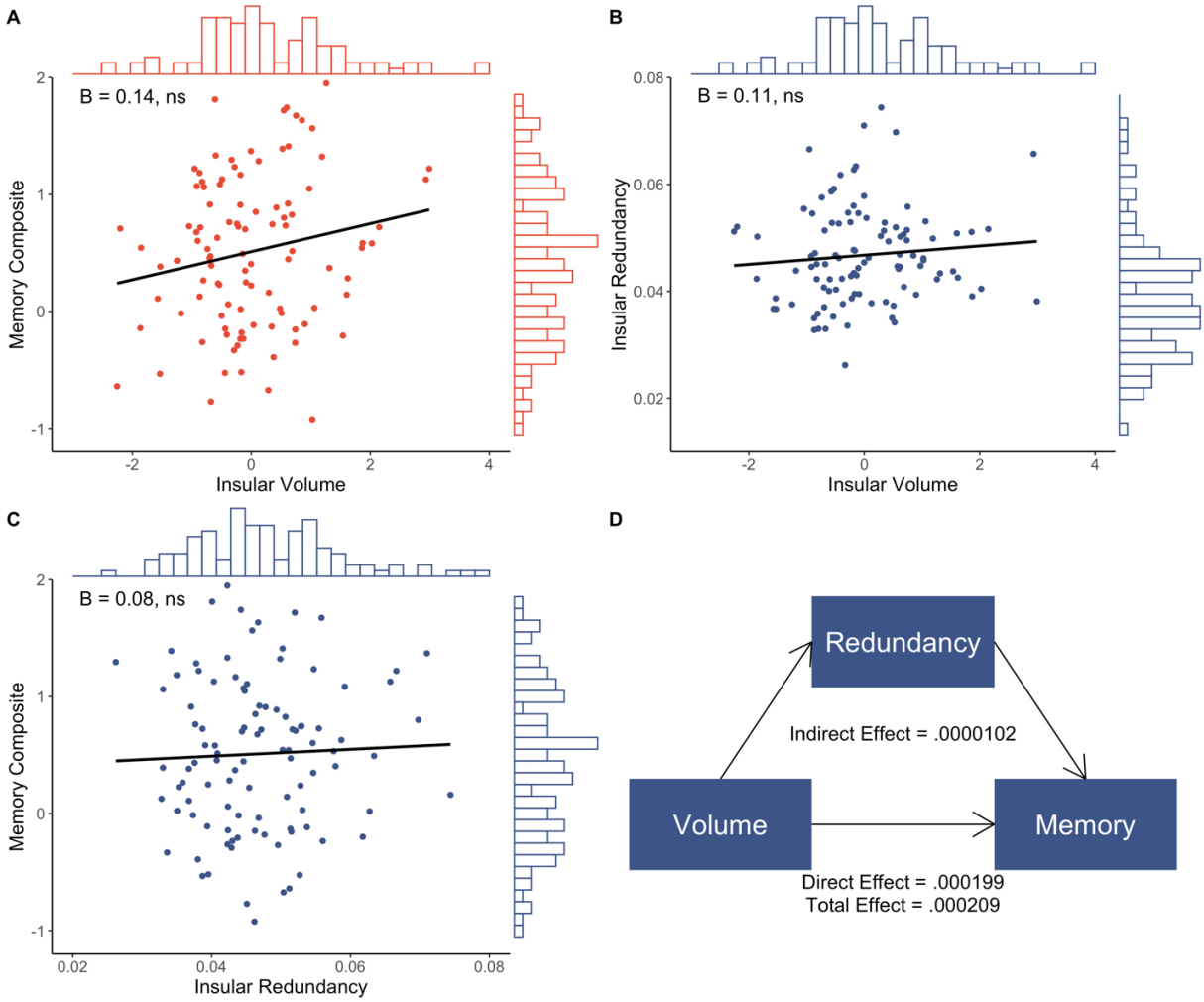

Figure 4. Relationships between insular volume, redundancy, and memory.

Whole sample regression of insular volume on memory composite score **(A)**, insular volume on insular redundancy **(B)**, and insular redundancy on memory composite score **(C)**, with histograms showing distribution of variable values and inset standardized beta coefficients. **D.** Mediation results from insular volume-redundancy-memory model.

Table 1

Participant characteristics by diagnosis

	CN (*n* = 27)	MCI (*n* = 75)	Test Statistic	*p*
Age	75.26 (6.51)	71.85 (6.51)	$t(100) = 2.33$	**.022**
Sex	15F/12M	36F/39M	$X^2(1) = 0.20$	.654
Education	16.19 (1.98)	16.15 (2.68)	$t(100) = 0.07$	.946
Aβ burden	8+/19−	43+/32−	$X^2(1) = 5.04$	**.025**
MMSE	28.74 (1.10)	27.99 (1.75)	$t(100) = 2.09$	**.039**
Memory	0.99 (0.57)	0.34 (0.59)	$t(100) = 4.93$	< **.001**
EF	0.87 (0.74)	0.43 (0.92)	$t(100) = 2.24$	**.027**

Note: Standard deviation given in parentheses; age and education given in years; CN = cognitively normal, MCI = mild cognitive impairment

Table 2

Linear regression output between hippocampal topological measures, volume, and cognition at the averaged density

	Redundancy-Volume			**Redundancy-Memory**			**Redundancy-EF**		
	β	*p*	R^2	β	*p*	R^2	β	*p*	R^2
All	0.27	**.022**	.025	0.34	**<.001**	.242	0.17	.052	.227
MCI	0.29	**.039**	.032	0.32	**.002**	.277	0.11	.280	.249

	Efficiency-Volume			**Efficiency-Memory**			**Efficiency-EF**		
	β	*p*	R^2	β	*p*	R^2	β	*p*	R^2
All	0.24	**.043**	.009	0.12	.209	.138	0.05	.608	.198
MCI	0.34	**.019**	.026	.096	.362	.184	−0.01	.893	.237

Note: Output from analyses using all participants (CN and MCI) and MCI only. β = standardized beta, R^2 = adjusted R^2, CN = cognitively normal, MCI = mild cognitive impairment, EF = executive function

Table 3

Mediation output at the averaged density

	Indirect Effect			Direct Effect		
Volume – Redundancy – Memory						
	β	**95% CI**	***p***	**β**	**95% CI**	***p***
All	1.32×10^{-4}	2.40×10^{-5}, 2.81×10^{-4}	**.013**	5.31×10^{-4}	1.83×10^{-4}, 9.25×10^{-4}	**.004**
MCI	1.08×10^{-4}	2.74×10^{-6}, 3.00×10^{-4}	**.038**	5.34×10^{-4}	1.64×10^{-4}, 9.20×10^{-4}	**.006**
Volume – Local Efficiency – Memory						
	β	**95% CI**	***p***	**β**	**95% CI**	***p***
All	2.29×10^{-5}	-6.06×10^{-5}, 1.31×10^{-4}	.562	6.40×10^{-4}	2.87×10^{-4}, 1.02×10^{-3}	**.001**
MCI	-2.58×10^{-8}	-1.38×10^{-4}, 1.07×10^{-4}	.968	6.42×10^{-4}	3.11×10^{-4}, 1.04×10^{-3}	**<.001**
Volume – Redundancy – Executive Function						
	β	**95% CI**	***p***	**β**	**95% CI**	***p***
All	9.63×10^{-5}	-2.27×10^{-5}, 2.79×10^{-4}	.122	3.18×10^{-4}	-1.56×10^{-4}, 7.86×10^{-4}	.184
MCI	6.11×10^{-5}	-7.29×10^{-5}, 3.02×10^{-4}	.417	2.54×10^{-4}	-3.04×10^{-4}, 7.62×10^{-4}	.373
Volume – Local Efficiency – Executive Function						
	β	**95% CI**	***p***	**β**	**95% CI**	***p***
All	9.90×10^{-6}	-1.10×10^{-4}, 1.61×10^{-4}	.841	4.05×10^{-4}	-8.57×10^{-5}, 8.88×10^{-4}	.099
MCI	-3.76×10^{-5}	-2.28×10^{-4}, 1.68×10^{-4}	.664	3.53×10^{-4}	-2.12×10^{-4}, 8.99×10^{-4}	.207

Note: Output from analyses using all participants (CN and MCI) and MCI only. β = unstandardized beta, CI = confidence interval, CN = cognitively normal, MCI = mild cognitive impairment